PARTITIONED ANALYSIS OF COUPLED SYSTEMS USING SUBCYCLING DEVICES IN FLUID-THERMAL INTERACTION PROBLEMS

A.M.P. Valli
L. Catabriga
avalli@inf.ufes.br
luciac@inf.ufes.br
Computer Science Departament, Federal Universiy of Espírito Santo
Av. Fernando Ferrani, s/n, 29060-900, Vitória - ES - Brazil
A.L.G.A. Coutinho
alvaro@nacad.ufrj.br
Department of Civil Engineering, COPPE, Federal University of Rio de Janeiro
PO Box 68506, 21945-970, Rio de Janeiro - RJ - Brazil
G.F. Carey
carey@cfdlab.ae.utexas.edu
Institute for Computational Engineering and Sciences, The University of Texas at Austin
201 E. 24th St., ACES 6.430, 1 University Station C0200, 78712-0227, Austin - TX - USA

Abstract. *This work investigates the use of partitioned analysis of coupled systems involving fluid-thermal interaction. Viscous flow is modeled by the incompressible 2D Navier-Stokes equations, with a forcing term that may depend on temperature, coupled to the transport of heat by convection and conduction. Of particular interesse in the present work is 2-D Rayleigh-Benard flows. The finite element flow formulation is based on a penalty Galerkin method and the transport equation utilizes a SUPG method. In our solution approach each equation of the coupled system is separately advanced in time. Interaction effects are accounted for by transmission and synchronization of coupled state variables, and we focus our attention on alternative algorithms and implementation possibilities using subcycling devices. Numerical results demontrate the efficiency of the subcycling procedure in reduzing the total computational effort to obtain the numerical solution.*

Keywords: *finite element, fluid-thermal interaction, subcycling devices, control timestep algorithms*

1. INTRODUCTION

When a thin horizontal fluid layer between two horizontal plates is heated from below, a temperature gradient is generated across the plates. At a critical Rayleigh number, circular convection cells set in - the heated fluid near the bottom begins to rise while the cooler fluid near the top descends. Buoyancy is a dominant component in driving this type of flow termed Rayleigh-Benard problem. To develop effective algorithms capable of high resolution transient flow and heat transfer computations, we need improved techniques. For example, domain decomposition strategies and parallel gradient-type iterative solution schemes have been developed and implemented with success for 3-D Rayleigh-Benard flow calculations by Carey et al. (1997). Also, with the evolution of the methodology and its extension to more complex classes of coupled problems, there has been an increasing need for other enhancements such as adaptive grid refinement and coarsening. Several adaptive timestepping selection strategies have been studied as a means to provide stable accurate transient (and steady state) solutions more efficiently (Winget and Hughes (1985); Coutinho and Alves (1996); Valli et al. (1998, 1999a,b)). The focus in our work is to investigate alternative algorithms and implementation possibilities using *subcycling* devices (Fellipa et al. (2001)) to demonstrate the efficiency of the partitioning procedure in reducing the total computational effort to obtain the numerical solution.

In the numerical integration of ordinary differential equations by implicit timestepping methods, a system of nonlinear equations has to be solved at every step. In general, it is common to use fixed-point iterations or modified Newton iterations. In the present work, we use fixed-point iterations given by successive approximations. The convergence rate of the iterative methods depends on the stepsize (Gustafsson and Soderlind (1997)), and the computational efficiency of the method can be measured by the total number of successive iterations to obtain the final solution. To improve efficiency, diminishing computational costs, it is necessary to control the convergence rate of the fixed point iterations. We consider the transient flow of a viscous incompressible fluid as described by the Navier-Stokes equations coupled to the heat transfer equation. The present algorithm employs a decoupled scheme, where the momentum and continuity equations are solved first, in each timestep, lagging the temperature in the forcing term. Then, the heat transfer equation is solved with the computed velocities as input. The finite element flow formulation is based on a penalty Galerkin method to enforce the incompressibility constraint, and the heat equation utilizes a SUPG method.

In the next section we briefly state the class of coupled viscous flow and heat transfer problems under investigation, the finite element formulation and the solution approach. Then, we describe two timestep control algorithms based on controlling either accuracy or the convergence rate of the successive iterations and the *subcycling* approach. Next, results of the classic Rayleigh-Benard problem are compared for fixed timestep, our control approaches and the partitioned procedure. Finally, some conclusions are given.

2. COUPLED VISCOUS FLOW AND TRANSPORT

Natural convection of an incompressible fluid can be driven by buoyancy forces due to temperature gradients. When a thin horizontal layer fluid between two horizontal plates is heated from below, a temperature gradient is generated across the plates. At critical Rayleigh number, circular convection cells set in - the heated fluid near the bottom begins to rise while the cooler fluid near to the top descends. Buoyancy is a dominant component in driving this type of flow termed Rayleigh-Benard problem. The dimensionless equations describing the

Rayleigh-Benard flows are

$$\frac{\partial \mathbf{u}}{\partial t} + \mathbf{u}\cdot\nabla\mathbf{u} - \nabla^2\mathbf{u} + \boldsymbol{\nabla} p = \frac{Ra}{Pr} T\mathbf{g} \qquad \text{in } \Omega \times I \tag{1}$$

$$\boldsymbol{\nabla}\cdot\mathbf{u} = 0 \qquad \text{in } \Omega \times I \tag{2}$$

$$\frac{\partial T}{\partial t} + \mathbf{u}\cdot\nabla T - \frac{1}{Pr}\nabla^2 T = 0 \qquad \text{in } \Omega \times I \tag{3}$$

where Ω is the flow domain, $I = [0, \bar{t}]$ is the time interval, $\mathbf{u} = (u, v)$ is the velocity vector, p is the pressure, T is the temperature, $Ra = \frac{\beta_T \Delta T g L^3}{\nu\alpha}$ is the Rayleigh number, β_T is the thermal coefficient, ΔT is the temperature difference for flows with heated or cooled walls, $\mathbf{g}$ is the gravity vector, L is a characteristic length scale of the flow, $\alpha = \frac{k}{\rho c_p}$ is the thermal diffusivity and $Pr = \frac{\nu}{\alpha}$ is the Prandtl number. Boundary conditions and initial conditions for temperature and velocities complete the mathematical statement of the problem. The finite element flow formulation is based on a penalty Galerkin method and the transport equation utilizes a SUPG formulation.

In the present work, we are only interested in the velocity solution and the associated coupled transport processes. Hence, for simplicity and convenience we use a penalty method to enforce the incompressibility constraint (Carey and Oden (1986); Carey and Krishnan (1984)). The penalty approach for the Navier-Stokes problem is designed to determine an approximate formulation involving only velocities and not pressures. Hence the size of the problem is reduced accordingly. Introducing a finite element discretization and basis on a uniform discretization Ω_h of quadrilateral elements, the semidiscrete projection of the penalized variational formulation of the Navier-Stokes equations (1), (2) leads to an non-linear semidiscrete system of ordinary differential equations, which is solved by successive approximations in the present study. We integrate the ODE system implicitly using a Crank-Nicolson scheme, and the resulting linear systems are solved using a direct frontal solver. Similarly, introducing a stabilized SUPG scheme for the temperature T, the resulting semi-discrete ODE system is also integrated implicitly using the Crank-Nicolson scheme, and here we also apply a frontal solver to find solutions of the resulting linear systems. More details of the finite element formulations can be found in Valli et al. (2002, 2001, 1999a, 1998).

Within each timestep we must solve a coupled nonlinear algebraic system associated with the discretized flow and transport equations. The main coupling between the flow and transport subsystems enters weakly through the dependence of the source term in the flow equations on the temperature and and the convective velocity in the temperature transport. Since the class of applications here does not involve high speed flow a corresponding iterative block decoupling of the subsystems within each timestep will be effective. That is, we can decouple the respective discretized flow and transport systems by a successive approximation scheme in which the source term is "lagged" in the flow equation and the computed velocity iterate is then used in the discretized transport subsystems. This successive approximation iteration may be repeated until convergence. In our experiments we consider one single step within each timestep.

In the application problems, we computed steady-state solutions using fixed timestep sizes and adaptive timestep sizes to test the efficiency of our PID controllers and the *subcycling* device to solve the related class of coupled problems. In the next section, we present briefly the PID controllers used and the *subcycling* device of partitioned analysis time stepping implemented.

3. TIME STEPPING STRATEGIES

3.1 Control Algorithms

Most timestep schemes are based on controlling accuracy as determined by truncation error estimates (e.g. Prediction-Modification-Correction). The objective of timestep selection is to minimize the computational effort to construct an approximate solution of a given problem in accordance with a desired accuracy. Gustafsson et al. (1988); Gustafsson (1991, 1994) showed that stepsize selection can be viewed as an automatic control problem with a PID controller defined as

$$\triangle t_{n+1} = (\frac{e_{n-1}}{e_n})^{k_P} (\frac{tol}{e_n})^{k_I} (\frac{{e_{n-1}}^2}{e_n e_{n-2}})^{k_D} \triangle t_n, \tag{4}$$

where tol is some input tolerance, e_n is the measure of the change of the quantities of interest in time t_n, and k_P, k_I and k_D are the PID parameters. Gustafsson and Soderlind (1997) establish a model for controlling the convergence rate of the iterative method that relates the convergence rate to the stepsize. Assuming that the stepsize is limited by the convergence rate of nonlinear iterations, the new stepsize should be chosen as

$$\Delta t_{n+1} = \frac{\alpha_{ref}}{\alpha} \Delta t_n \tag{5}$$

where α_{ref} is a reference rate of convergence and α is an estimated rate of convergence. Now the controller tries to keep the estimated convergence rate as close as possible to a reference value, α_{ref}. In general, any value $0.2 < \alpha_{ref} < 0.4$ would be acceptable, and $\alpha_{ref} \approx 0.2$ gives performance near to optimal (Gustafsson and Soderlind (1997)). The estimated rate of convergence is calculated using three consecutive iterates for the velocities, $\mathbf{u}_{n-2}$, $\mathbf{u}_{n-1}$, and $\mathbf{u}_n$, as follows

$$\alpha = \max \alpha_n = \max_n \frac{\|\mathbf{u}_n - \mathbf{u}_{n-1}\|}{\|\mathbf{u}_{n-1} - \mathbf{u}_{n-2}\|} \tag{6}$$

It is necessary to coordinate the convergence control algorithm (5) with the stepsize control strategy (4) so that efficiency is maintained. Based on equations (5) and (6), we propose two timestep control algorithms.

The first control uses changes in velocities and temperature, and can be motivated on the need to control accuracy with respect to time in the specific solution variables. The **Control 1** is defined by

$$\triangle t = \left(\frac{e_{n-1}}{e_n}\right)^{k_P} \left(\frac{1}{e_n}\right)^{k_I} \left(\frac{{e_{n-1}}^2}{e_n e_{n-2}}\right)^{k_D} \triangle t_{prev} \tag{7}$$

with

$$e_n = \max(e_u, e_T), \tag{8}$$

where

$$e_u = \frac{e_u^*}{\text{tol}_u} \qquad e_u^* = \frac{\|\mathbf{U}^n - \mathbf{U}^{n-1}\|}{\|\mathbf{U}^n\|} \tag{9}$$

$$e_T = \frac{e_T^*}{\text{tol}_T} \qquad e_T^* = \frac{\|\mathbf{T}^n - \mathbf{T}^{n-1}\|}{\|\mathbf{T}^n\|} \tag{10}$$

and Δt represents the new timestep size, $\triangle t_{prev}$ is the timestep size at the previous step, and tol_u, tol_T and tol_c are user supplied tolerances corresponding to the normalized changes in velocities and temperature vectors, respectively.

In the second control, the size of the timestep is limited by the changes in the kinetic energy or by the rate of convergence of the successive approximations. The **Control 2** is given by

$$\Delta t = \min(\Delta t_\alpha, \Delta t_r), \tag{11}$$

where

$$\Delta t_\alpha = \frac{\alpha_{ref}}{\alpha}\,\Delta t_{prev} \tag{12}$$

$$\triangle t_r = \left(\frac{e_{n-1}}{e_n}\right)^{k_P}\left(\frac{1}{e_n}\right)^{k_I}\left(\frac{{e_{n-1}}^2}{e_n e_{n-2}}\right)^{k_D}\triangle t_{prev} \tag{13}$$

and

$$e_n = \frac{e_K^*}{\text{tol}_K}, \qquad e_K^* = \frac{\|K^n - K^{n-1}\|}{\|K^n\|}, \qquad K = \int_\Omega \frac{(u^{*2} + v^{*2})}{2}\,d\Omega. \tag{14}$$

Here, tol_K is a given tolerance corresponding to the normalized changes in kinetic energy, and u^* and v^* are the nondimensional velocity components. The motivation in choosing this control for the kinetic energy is related to an interest in the qualitative behavior of the solution as different cell structures, steady-state solutions, periodic solutions or aperiodic solutions arise.

The algorithm for controlling the timestep has two main parts. First, a step size is assumed, and using the newly computed solution, an *a posteriori* estimate is made of the error in the step. Second, this error measure is used to accept or reject the solution and modify the timestep accordingly. If the error is unacceptable, the new solution is discarded and we restart the time integration in the previous step with a a scaled timestep size based on the magnitude of the error relative to the tolerance. In our algorithm, if the sequence of iterates of the nonlinear system is converging at a slow rate, the timestep is also rejected. That is, if the number of successive approximations nsa is greater than the maximum number of successive approximations allowed nsa_{max}, the stepsize is rejected. If the error is acceptable, a new timestep is calculated using (7) or (11) and we proceed with the time integration.

To prevent an excessive growth or reduction of the step size $\triangle t$, we supply timestep limits $\triangle t_{min}$ and $\triangle t_{max}$ which limit the control signal (Franklin et al. (1994)). We performed parametric studies for different values of PID parameters (k_P, k_I, k_D) for test problems in Valli et al. (2002, 1998), to verify whether the PID controller is robust or not. Although feedback control theory provides techniques to choose PID parameters, robustness is required when a general method is used for a wide range of different situations. The controller was found to be very robust, allowing us to fix the values of the PID parameters, $k_P = 0.075$, $k_I = 0.175$ and $k_D = 0.01$, for all the numerical experiments performed subsequently.

3.2 Partitioning in time

The coupled system investigated in this work involves fluid-thermal interaction, and the fields are discretized in space and time. Because we are simulating different physical subsystems, it is possible that the response to each process occurs at different time scales. For example, in aircraft aeroelasticity, structural motions are typically dominated by low frequency vibration modes. On the other hand, the fluid response must be captured in a smaller time scale because of nonstationary effects involving shocks, vortices and turbulence (Fellipa et al. (2001)). Thus the

use of a smaller time scale for the fluid is natural. This partitioning device is called *subcycling* and it will be used here to simulate the fluid-thermal interaction.

In our original algorithm, we calculate a sequential staggered solution of the problem: first we solve the momentum and continuity equations, lagging the temperature in the forcing term; then, the transport equation is solved with the computed velocities as input. This zigzagged picture of interfield data transfers between the two programs is depicted in Figure 1. We can have fixed or adaptive timestep given by the PID controllers to advance in time. In this approach, the velocities and temperature are updated at each timestep. Now, the idea is modify this algorithm to include the *subcycling* device and evaluate the cost and accuracy of the new solutions.

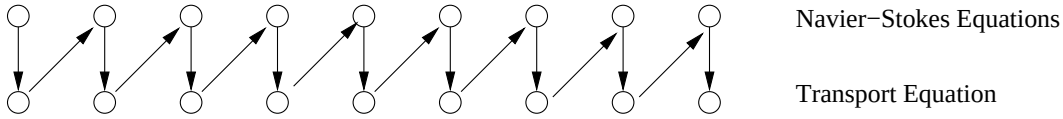

Figure 1: Sequential staggered solution of the problem.

In the partitioned solution approach, the systems are spatially decomposed into partitions, and the solution is separately advanced in time over each partition. In the *subcycling* technique, different timestep intervals will be used to solve the two problems, as sketched in Figure 2. Now, we solve the momentum and continuity equations lagging the temperature in the forcing term; then, the transport equation is solved for a fixed number of steps with the last computed velocities as input. After one cycle, the velocities are computed with the last updated temperature. At the beginning of the process, the velocities and temperature are updated at each step for a small number of fixed step sizes.

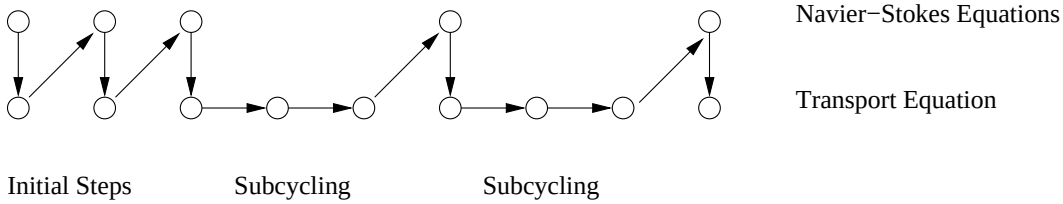

Figure 2: *Subcycling* device on the transport equation.

We define the ratio of thermal to fluid timestep as being $np : 1$, and we use a smaller time scale for the heat calculations. After np temperature calculations on the transport equation, the last updated temperature enters in the buoyancy term of the momentum equation and the new velocities are calculated. Then, we calculated the new temperature with the last update velocities and an new cycle begins. Interaction effects are accounted for by transmission and synchronization of coupled state variables. In the next section, two problems are solved to compared the efficiency of the algorithms proposed here.

4. RESULTS

Our first example involves natural convection in a unit square $\Omega = [0, 1] \times [0, 1]$ with temperatures $T = 1$, $T = 0$ on the left and right walls respectively, adiabatic top and bottom wall (no free surface), with $Pr = 0.71$ and different Rayleigh numbers, Ra, of 10^3, 10^4 and 10^5. The computed Nusselt number at the left wall (Nu_0 = $\int_0^1 q dy$, where q is the heat flux), and the stream function at the midpoint (ψ_{mid}) are compared to the results from Davis (1968, 1983a,b). The stream function contours and temperature contours for $Ra = 10^3$, $Ra = 10^4$ and

$Ra = 10^5$ are shown in Figure 3 and Figure 4, respectively. The contour values are the same as in Davis (1983b) and show excellent agreement with his results.

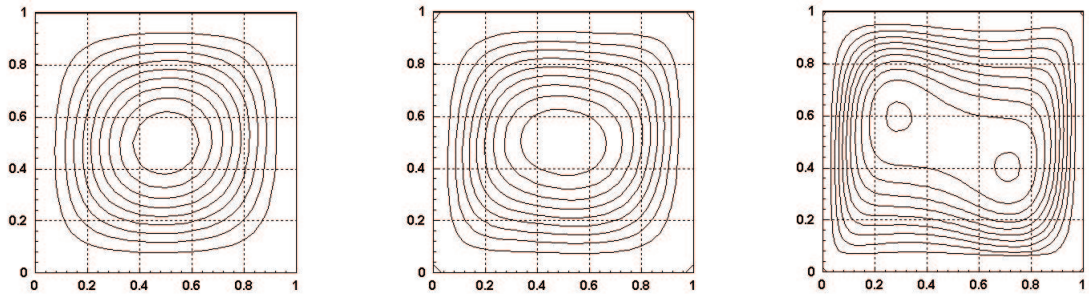

Figure 3: Stream functions contours for Ra = 10^3 (equally spaced (0.1174) between -1.0566 and 0), Ra = 10^4 (equally spaced (0.5071) between -4.5639 and 0) and Ra = 10^5 (equally spaced (0.9607) between -9.507 and 0).

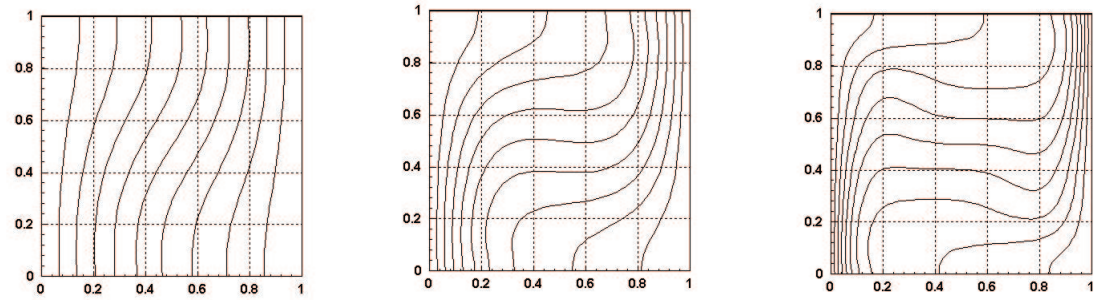

Figure 4: Temperature contours for $Ra = 10^3$, $Ra = 10^4$ and $Ra = 10^5$ (equally spaced (0.1) between 1 and 0).

The approximate velocities and temperature are calculated using 9-node isoparametric quadrilaterals elements in a uniform mesh of 16×16 elements at $Ra = 10^3, 10^4$ and 32×32 elements at $Ra = 10^5$. The initial timestep size in all cases is chosen to allow convergence of the successive iterations at the beginning of the process. That is, if we start with a timestep size greater than the initial timesteps chosen here, the successive approximation iterations failed to converge after a few time steps. We start with a timestep size of 0.01 at $Ra = 10^3, 10^4$ and 0.001 at $Ra = 10^5$. We assume that the steady-state occurs when the kinetic energy at two different time steps reaches a relative difference less than a given tolerance, tol_{st}. We establish that the steady-state occurs when $tol_{st} = 10^{-4}$ at $Ra = 10^3$ and $tol_{st} = 10^{-3}$ at $Ra = 10^4, 10^5$. The results are shown in Table 1, and the agreement for all cases are good with percentage errors no more than 1.5% in all quantities as shown in Table 2. Observe that the differences increase as Ra increases due to the growing difficulty of the problem.

Now we compare the computational effort to calculate the solution using fixed timesteps, the PID controllers, and the *subcycling*. The computational effort is measured by the total number of successive approximations needed to calculate the velocity field using one of the approaches divided by the number of successive approximations obtained using a fixed timestep size. For each case, we calculate the total number of successive approximations, nsa, and the computational effort, c_{effort}. The results are shown in Table 3.

For $Ra = 10^3$, we start with a minimum timestep size of 0.01, and we allow a maximum timestep size of 0.1. We define a tolerance of 0.1 for changes in nodal velocities and temperature. The tolerance corresponding to the normalized changes in kinetic energy is equal to one.

Table 1: Comparison of specific results to benchmark case

	Fixed Δt		Control 1		Control 2		Subycling		Benchmark	
Ra	Nu_0	ψ_{mid}	Nu_0	ψ_{mid}	Nu_0	ψ_{mid}	Nu_0	ψ_{mid}	Nu_0	ψ_{mid}
10^3	1.118	1.175	1.117	1.173	1.117	1.174	1.117	1.174	1.117	1.174
10^4	2.255	5.067	2.236	5.077	2.246	5.064	2.266	5.096	2.238	5.071
10^5	4.550	9.134	4.518	9.036	4.553	9.120	4.552	9.114	4.509	9.111

Table 2: Percentage errors

	Fixed Δt		Control 1		Control 2		Subycling	
Ra	Nu_0	ψ_{mid}	Nu_0	ψ_{mid}	Nu_0	ψ_{mid}	Nu_0	ψ_{mid}
10^3	0.1	0.1	0.2	0.1	0.0	0.0	0.0	0.0
10^4	0.8	0.1	0.1	0.1	0.4	0.1	1.3	0.5
10^5	0.9	0.3	0.2	0.8	1.0	0.1	0.9	0.0

Table 3: Computational effort for the natural convection problem.

	Fixed Δt		Control 1		Control 2		Subycling	
Ra	nsa	c_{effort}	nsa	c_{effort}	nsa	c_{effort}	nsa	c_{effort}
10^3	58	1.0	32	0.55	24	0.41	25	0.43
10^4	56	1.0	47	0.84	45	0.80	29	0.52
10^5	363	1.0	260	0.72	189	0.52	134	0.37

The reference rate of convergence is equal to 0.2. We can observe in Table 3 that the number of successive approximations necessary to calculate the approximate solutions is reduced for all approaches. However, Control 2 presents the best results. We obtain the solution with 24 successive iterations using Control 2, and we need 58 iterations with the fixed timestep size. Thus, we are able to calculate the solution 2.4 times faster using Control 2 without any significant loss of accuracy. For Control 2, the choice of the timestep is dominated by the changes in the kinetic energy in all iterations. Note that the *subcycling* device also reduced significantly the number of successive approximations and the values of the Nusselt number and the stream function are the same calculated using Control 2.

For $Ra = 10^4$, we start with a minimum timestep of 0.01, and we allow a maximum timestep size of 0.1. We define tolerances of 0.2, 0.1 and 0.5 for changes in nodal velocities, temperature and kinetic energy, respectively. The reference rate of convergence is equal to 0.19. Here we also improve efficiency for all approaches, reducing the number of successive approximations necessary to calculate the approximate solutions. Control 1 and Control 2 are equivalent in terms of efficiency. The choice of the timestep in Control 2 is dominated by the convergence rate of the successive iterations, with only two time iterations limited by the changes in the kinetic energy. The *subcycling* device presents the best results, and the solution is calculated 1.93 times faster. However, the results for the *subcycling* device are less accurate.

For $Ra = 10^5$, we start with a minimum timestep size of 0.001, and we allow a maximum timestep size of 0.1. We define a tolerance of 0.1 for changes in nodal velocities and tempera-

ture. The tolerance corresponding to the normalized changes in kinetic energy is equal to one. The reference rate of convergence is equal to 0.25. Now, Control 2 is dominated by the changes in the kinetic energy, with only 4 iterations calculated according to the convergence rate of the successive iterations. All approaches reduce the number of successive approximations to obtain the solution, but the *subcycling* device gives the best result. The total number of successive approximations obtained by Control 1 can be reduced if we define large tolerances for changes in nodal velocities and temperature. However, the results will loose accuracy.

In the second example, we consider flow in a rectangular container of length 4 times the height with Pr = 0.72 and Ra = 30000. The temperatures on the bottom surface and top surface are T_h = 1 and T_c = 0, respectively. The approximate velocity and temperature are calculated using biquadratic shape functions with a grid of 32 $\times$ 8 elements, with the PID timestep selection and the *subcycling* device. We consider the steady-state problem and the computed vector field and temperature contours are shown in Figure 5. There are six recirculation cells, and the results agree with those in Griebel et al. (1998).

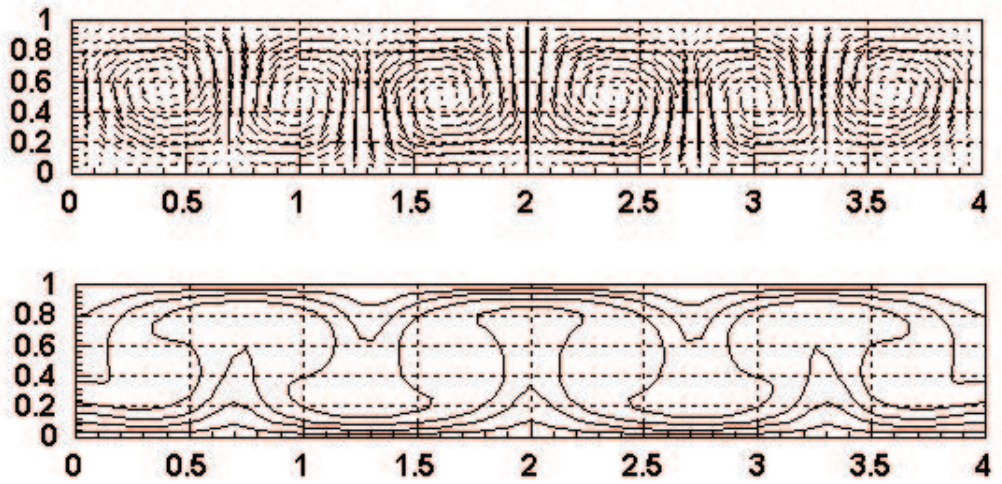

Figure 5: Vector field and temperature contours for the flow in a container with aspect ratio 4:1

The steady-state solution is obtained at $\tau_u = \tau_T = 10^{-3}$, and we set a tolerance of 0.01 for changes in nodal velocities and temperature. We start with a timestep size of 0.001, and we allow minimum and maximum time steps of 0.001 and 0.5, respectively. This starting timestep is the largest for which we obtained convergence in the successive iterations. The reference rate of convergence of nonlinear iterations is chosen equal to 0.35 in this example. As we can see in Table 4, we obtain the solutions with a reduced number of successive approximation iterations using the two controllers and the *subcycling* device. Control 2 gives a smaller computational effort than Control 1, however the *subcycling* device gives the best result. With a fixed timestep size of 0.001 we need 731 iterations, and only 230 iterations when the *subcycling* device is applied. In this case, the solution is obtained 3.2 times faster. Figure 6 compares the streamlines obtained with fixed timesteps and the *subcycling* device. As we can see, the solutions agree very well.

5. CONCLUSION

Since the class of coupled system investigated in this work involves fluid-thermal interaction, it is possible that the response to each process occurs at different time scales. Thus the use of a *subcycling* device to simulate the problem is natural. In the partitioned solution ap-

Table 4: Results for the problem using the controllers, fixed timestep sizes and the *subcycling* device.

	Fixed Δt	Control 1	Control 2	Subycling
nsa	731	643	380	230
c_{effort}	1	0.88	0.52	0.31

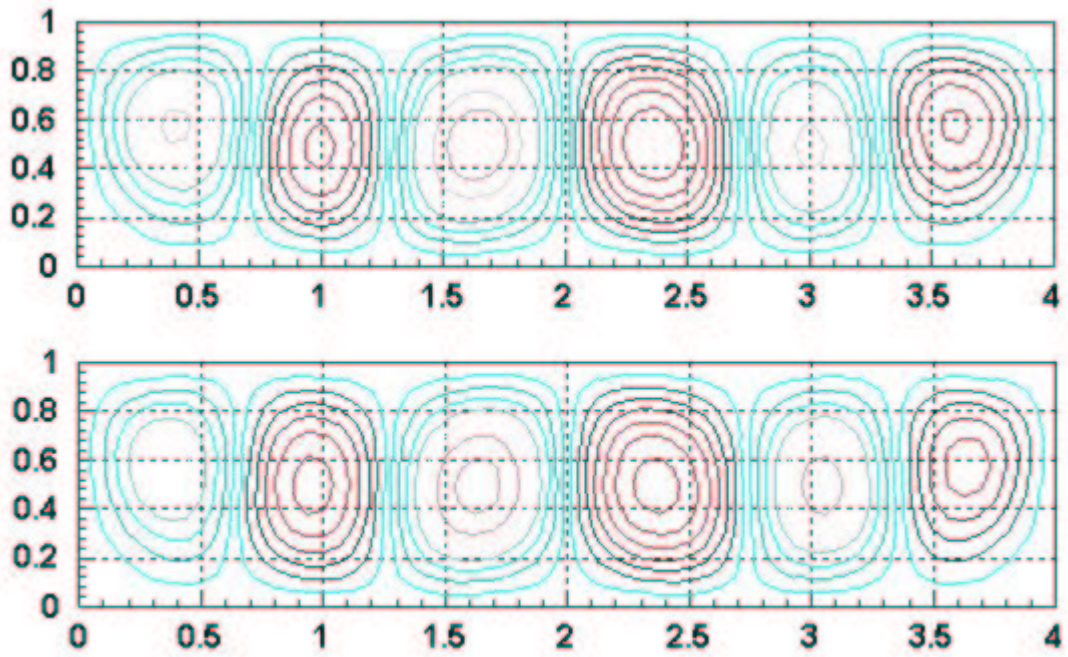

Figure 6: Streamlines for the flow in a container using fixed timestep sizes (top) and the *subcycling* device (bottom)

proach, the solution is separately advanced in time over each partition chosen in accordance with physical or computational characteristics. In this work we use two adaptive timestep selection schemes based on feedback control theory and a partitioning device to increase the robustness of our finite element formulation of coupled incompressible viscous flow and transient heat transfer. We solved Rayleigh-Benard flows with different parameters that influence the numerical experiments. The finite element flow formulation is based on a penalty Galerkin method and the transport equations utilize a SUPG formulation. The algorithm employs an iteratively decoupled scheme. In the application problems, we were interested in obtaining steady-state using the *subcycling* device and compare with the solutions obtained using fixed timestep sizes and adaptive timestep sizes to test the efficiency of this partitioning device to solve the related class of coupled problems.

The efficiency of the *subcycling* device was verified in the numerical simulations of the Rayleigh-Benard problems. The computational effort was measured by the total number of successive approximations needed to calculate the velocity field using one of the controllers or the *subcycling* device divided by the number of successive approximations obtained using a fixed timestep size. We observed that the number of successive approximations necessary to calculate the approximate solutions is reduced for all approaches, and the *subcycling* device

and Control 2 presented the best results. For example, in the second test problem the solution is obtained 3.2 times faster using the *subcycling* device and this solution agrees very well with the solution using fixed timestep sizes. Future studies include to investigate partitioned analysis procedures for coupled systems in conjunction with control timestep algorithms. The idea is to use the PID controllers to advance in time over the transport partition and synchronize with the calculations on the Navier-Stokes partition.

Acknowledgments

This work is partly supported by CAPES, under Grant CAPES/UT N° 11/04, and by CNPq and Federal University of Espírito Santo (UFES), under PIBIC program.

REFERENCES

Carey, G., Harlé, C., McLay, R., & Swift, S., 1997. MPP solution of Rayleigh-Benard-Marangoni flows. In *Supercomputing 97*, pp. 1–13, San Jose, CA.

Carey, G. & Krishnan, R., 1984. Penalty finite element methods for the Navier–Stokes equations. *Comput. Meths. Appl. Mech. Engrg.*, vol. 42, pp. 183–224.

Carey, G. & Oden, J., 1986. *Finite Elements: Fluid Mechanics*, volume 6. Prentice–Hall, Inc., Englewood Cliffs, NJ.

Coutinho, A. & Alves, J., 1996. Parallel finite element simulation of miscible displacements in porous media. *SPE Journal*, vol. 4, n. 1, pp. 487–500.

Davis, G. D. V., 1968. Laminar natural convection in a enclosed rectangular cavity. *Int. J. Heat Mass Transfer*, vol. 11, pp. 1675–1693.

Davis, G. D. V., 1983a. Natural convection in a square cavity: A comparison exercise. *Int. J. Num. Meth. Fluids*, vol. 3, pp. 227–248.

Davis, G. D. V., 1983b. Natural convection of air in a square cavity: A benchmark numerical solution. *Int. J. Num. Meth. Fluids*, vol. 3, pp. 249–264.

Fellipa, C., Park, K., & Farhat, C., 2001. Partitioned analysis of coupled system. *Comp. Meths, Appl. Mech. Engrg.*, vol. 190, pp. 3247–3270.

Franklin, G., Powell, J., & Emami-Naeini, A., 1994. *Feedback Control of Dynamic Systems*. Addison-Wesley Publishing Company.

Griebel, M., Dornseifer, T., & Neunhoeffer, T., 1998. *Numerical Simulation in Fluid Dynamics - A Practical Introduction*. SIAM, Philadelphia, PA.

Gustafsson, K., 1991. Control theoretic techniques for stepsize selection in explicit Runge-Kutta methods. *ACM TOMS*, vol. 17, pp. 533–554.

Gustafsson, K., 1994. Control theoretic techniques for stepsize selection in implicit Runge-Kutta methods. *ACM TOMS*, vol. 20, pp. 496–517.

Gustafsson, K., Lundh, M., & Soderlind, G., 1988. A PI stepsize control for the numerical solution for ordinary differential equations. *BIT*, vol. 28, pp. 270–287.

Gustafsson, K. & Soderlind, G., 1997. Control strategies for the iterative solution of nonlinear equations in ODE solvers. *SIAM J. Sci. Comput.*, vol. 18, n. 1, pp. 23–40.

Valli, A., Carey, G., & Coutinho, A., 1998. Finite element simulation and control of nonlinear flow and reactive transport. In *Proc. 10th Int. Conf. Finite Element in Fluids*, pp. 450–455, Tucson, Arizona.

Valli, A., Carey, G., & Coutinho, A., 2002. Control strategies for timestep selection in simulation of coupled viscous flow and heat transfer. *Communications in Numerical Methods in Engineering*, vol. 18, pp. 131–139.

Valli, A., Catabriga, L., & Coutinho, A., 2001. Acceleration strategies for solution of euler equations using an edge-based supg formulation with shock-capturing. In *ECCOMAS Computational Fluid Dynamics 2001 Conference CD-ROM*, Swansea, Wales, UK.

Valli, A., Coutinho, A., & Carey, G., 1999a. Adaptive control for time step selection in finite element simulation of coupled viscous flow and heat transfer. In *European Conference on Computational Mechanics CD-ROM*, Munchen, Germany.

Valli, A., Coutinho, A., & Carey, G., 1999b. Adaptive stepsize control strategies in finite element simulation of 2D Rayleigh-Benard-Marangoni flows. In *15th Brazilian Congress on Mechanical Sciences CD-ROM*, Águas de Lindóia, SP, Brazil.

Winget, J. & Hughes, T., 1985. Solution algorithms for nonlinear transient heat conduction analysis employing element-by-element iterative strategies. *Comput. Methods Appl. Mech. and Engrg.*, vol. 52, pp. 711–815.